

Ordering of droplets and light scattering in polymer dispersed liquid crystal films

A D Kiselev¹, O V Yaroshchuk² and L Dolgov²

¹ Chernigov State Technological University, Shevchenko Street 95, 14027 Chernigov, Ukraine

² Institute of Physics of NASU, prospekt Nauki 46, 03028 Kyïv, Ukraine

E-mail: kisel@mail.cn.ua

Received 1 June 2004, in final form 19 August 2004

Published 1 October 2004

Online at stacks.iop.org/JPhysCM/16/7183

doi:10.1088/0953-8984/16/41/002

Abstract

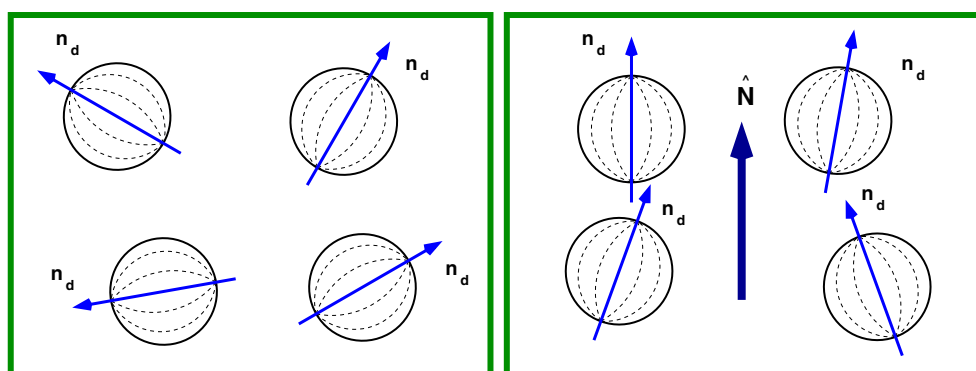
We study the effects of droplet ordering in initial optical transmittance through polymer dispersed liquid crystal (PDLC) films prepared in the presence of an electrical field. The experimental data are interpreted by using a theoretical approach to light scattering in PDLC films that explicitly relates optical transmittance and the order parameters, characterizing both the orientational structures inside bipolar droplets and orientational distribution of the droplets. The theory relies on the Rayleigh–Gans approximation and uses the Percus–Yevick approximation to take into account the effects due to droplet positional correlations.

(Some figures in this article are in colour only in the electronic version)

1. Introduction

Polymer dispersed liquid crystal (PDLC) materials have attracted considerable interest for both technological and more fundamental reasons. There are numerous existing and future applications of PDLC systems in optical displays, light shutters, filters and other optical elements [1–4]. Electro-optical devices based on two- and three-dimensional arrays of polymer-encapsulated nematic liquid crystal [5] also offer considerable promise for large-area flexible displays that can be arranged on plastic substrates [6].

PDLC films consist of randomly distributed micrometre-sized liquid crystal (LC) droplets embedded in an isotropic polymer matrix. The droplets are typically filled with a nematic liquid crystal (NLC). Optical characteristics of such birefringent nematic droplets differ from those of the surrounding polymer matrix and the droplets can be viewed as optically anisotropic inhomogeneities which scatter light incident upon them. Much of the fundamental interest in PDLC materials directly stems from their inhomogeneous nature, allowing the effects of spatial confinement on properties of liquid crystalline phases to be explored.

(a) Off state with $Q = 0$ (b) On state with $Q \approx 1$ **Figure 1.** (a) Random and (b) uniaxially anisotropic orientational distributions of bipolar droplets.

Optical transmittance of PDLC films is mostly determined by light scattering properties of NLC droplets that crucially depend on NLC orientational structure. This structure can be influenced by an external electrical field which reorients the NLC directors inside the droplets and thereby light scattering in the film appears to be governed by the field. This mechanism underlies the mode of operation of PDLC films that, under certain conditions, can be switched from an opaque to a clear state by applying an electric voltage.

Schematic representation of the field effect on the orientational structure is given in figure 1. The zero-field case in which orientation of NLCs is randomly distributed over the droplets is shown in figure 1(a). As is illustrated in figure 1(b), in the presence of a field, the NLC directors align along the prescribed direction \hat{N} . When the polymer index of refraction, n_p , and the ordinary refractive index of the NLCs, $n_{lc}^{(o)}$, are matched, the PDLC film in the on state is almost transparent for waves propagating along the voltage induced anisotropy axis \hat{N} .

Optical switching contrast, which is the ratio of the transmittance in the on state and the initial (zero-field) transmittance, is an important characteristic of the PDLC film. High switching contrast can be achieved by reducing the zero-field transmittance of the PDLC film and, for this purpose, the film should be prepared so as to maximize the optical contrast between the polymer and the NLC.

Typically, the extraordinary refractive index $n_{lc}^{(e)}$ is the largest value of the NLC refractive index and $n_{lc}^{(o)} \approx n_p < n_{lc}^{(e)}$. So, for light normally incident upon the film, in-plane alignment of the NLC inside the droplets will enhance scattering efficiency. The experimental procedures for stimulating NLC molecules to be aligned in the plane of the PDLC film were suggested in [1, 7, 8]. In these methods the film of the PDLC precursor was subjected to external fields (mechanical pressure, light, electrical and magnetic fields) during the phase separation.

In this paper we present both experimental and theoretical results for initial transmittance of PDLC films prepared in the presence of an electrical field applied across the film of the PDLC precursor. In this case the voltage will align NLC molecules perpendicular to the film thus reducing the switching contrast. We are, however, primarily interested in studying the relation between the optical transmittance of a PDLC film and the order parameters characterizing both the orientational structures inside the droplets and the overall anisotropy of the film.

To this end, we need to have a theory that explicitly relates the order parameters and the transmittance to interpret the experimental data. In [9, 10] the theory by Kelly and Palfy-Muhoray [11], that studied the electrical field induced effects in light scattering by an ensemble

of bipolar droplets, has been used to discuss the order parameter effects in optical transmittance through a PDLC film.

In the present paper these effects will be studied by using a more comprehensive approach that takes into account interference effects caused by droplet positional correlations. As in [12], for this purpose, we shall use the Percus–Yevick approximation. We also combine the effective medium theory [13] with the low concentration approximation to account for the dependent scattering effects.

The paper is organized as follows. In section 2, we give the necessary details on the experimental procedure used in this study and describe the morphology of the PDLC system under consideration. We present the experimentally measured dependencies of the zero-field transmittance and the transmittance in the saturated on state on the voltage U_{uv} applied across the film during UV polymerization.

Our theoretical considerations are presented in section 3. We characterize NLC director structures inside the bipolar droplets and the orientational distribution of the bipolar axis by the bipolar order parameter Q_d and the order parameter Q . Then we compute the effective dielectric constant and use the Rayleigh–Gans approximation to evaluate the scattering cross section of a bipolar droplet embedded in the effective medium. After averaging the cross section over both positions and orientation of bipolar droplets we derive the scattering mean free path and the optical transmittance. Dependencies of the transmittance on the order parameters at different droplet sizes are calculated numerically.

In section 4, we draw together and discuss our experimental and theoretical results. Using the theory we estimate the order parameters in the off and the on states from the experimental data. The value of the bipolar order parameter Q_d is found to be about 0.85. For samples prepared with no applied voltage, the order parameter Q turns out to be very close to zero. This order parameter rapidly grows and saturates as the voltage U_{uv} increases. Concluding remarks are given in section 5.

2. Experimental details

In this section we describe the experimental procedures used to prepare the PDLC films and to measure the optical transmittance of the samples in the zero-field and the saturated states. The key experimental results essential for subsequent theoretical treatment are presented in section 2.3.

Specifically, we characterize the morphology of the PDLC samples and the orientational structure inside NLC droplets. These results suggest that the PDLC system under consideration can be modelled as a collection of bipolar droplets. We also give the estimates for the droplet size and the droplet volume fraction that will be used as input parameters needed to evaluate the order parameters from the data on the optical transmittance.

2.1. Sample preparation

NLC mixture E7 from Merck and UV curable adhesive POA65 from Norland Inc. (USA) were used to prepare the composite. PDLC systems based on these components have been studied intensively [8, 14–17].

The components were thoroughly mixed. The content of LC and polymer precursor in the mixture was $c_p = 60$ wt% and $c_{lc} = 40$ wt%, respectively. The mixing was performed under red light so as to avoid early polymerization of POA65. The prepared mixture was sandwiched between two glass slabs covered with ITO on the inner side. The cell gap was maintained by spacer balls 20 μm in size. The substrates were pressed and glued with a epoxy glue.

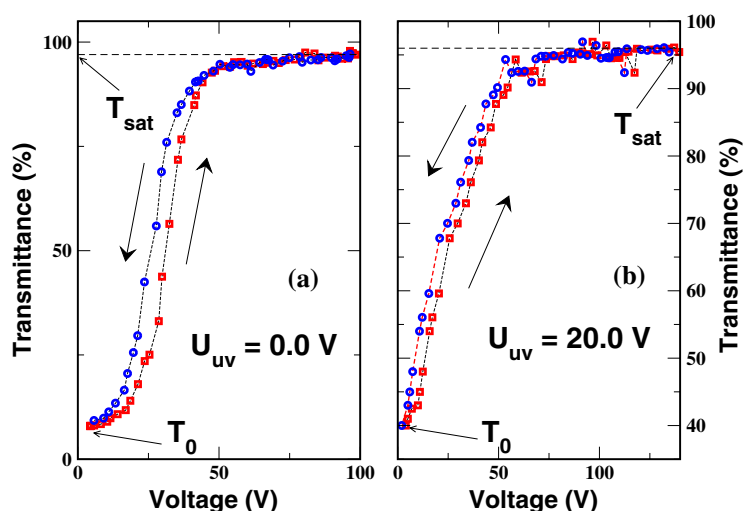


Figure 2. T - U dependences for two PDLC samples prepared at (a) $U_{uv} = 0$ V and (b) $U_{uv} = 20$ V. Arrows indicate an increase and a decrease of the applied voltage U .

In order to stimulate polymerization-induced phase separation leading to the formation of PDLC layers the samples were irradiated with the light from mercury lamp. The intensity and the time of irradiation were 100 mW cm^{-2} and 20 min, respectively.

The samples were subjected to the electrical field U_{uv} of the frequency $f = 2$ kHz during UV polymerization. The voltages $U_{uv} = 0, 2, 10, 20, 50$ and 100 V were applied across the samples to prepare PDLC layers with varying orientational distribution of droplets and, as a result, initial transmittance. The difference in transmittance was visible even to the human eye.

SEM measurements were carried out using device S-2600N from Hitachi. For performing the measurements the samples were treated as follows. One glass slab was removed and the remaining part of the sample was immersed into ethanol of purity 98% for 24 h. Then the sample was taken out from ethanol, dried and coated with gold.

2.2. Optical transmittance

Optical transmittance T versus applied voltage U curves were measured at room temperature using the computer conjugated measuring system previously described in [18]. The sample transmittance was defined as the ratio:

$$T = \frac{I_{\text{out}}}{I_{\text{in}}}, \quad (1)$$

where I_{in} is the intensity of the normally incident light with the wavelength $\lambda = 635$ nm and I_{out} is the intensity of the light transmitted through the sample. Following usual procedure, the non-scattered light and the light scattered within the angle of 2° were detected with a photodiode. The T - U curves were measured at both increasing and decreasing voltage. In this process, the voltage was varied from 0 to 100 V, whereas the frequency was fixed at 2 kHz. Typical T - U curves are shown in figure 2. As is indicated, the curves provide transmittance in the initial zero-field state (T_0) and in a state of saturation reached at sufficiently large voltages (T_{sat}).

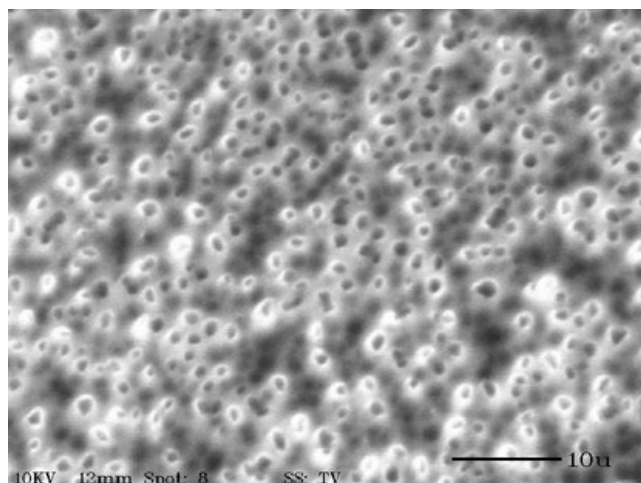


Figure 3. SEM image of the PDLC layer ($c_p = 60$ wt%, $c_{lc} = 40$ wt%).

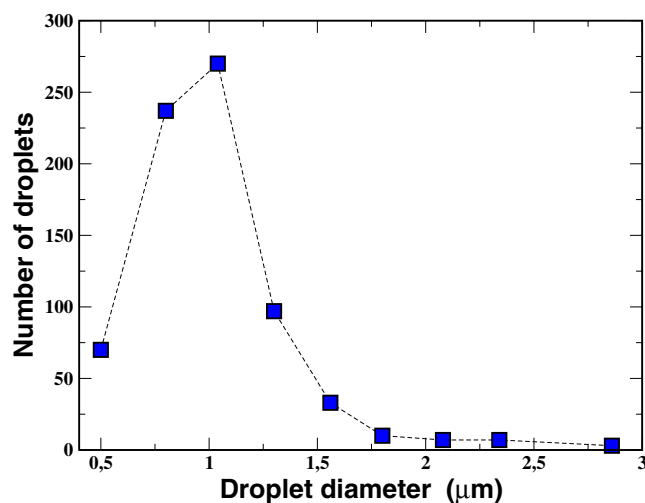


Figure 4. Distribution of droplet sizes in the PDLC layer ($c_p = 60$ wt%, $c_{lc} = 40$ wt%).

2.3. Experimental results

A typical SEM image and the corresponding distribution of droplet sizes are shown in figures 3 and 4, respectively. It is seen that the preparation procedure yields the well-known ‘Swiss cheese’ PDLC morphology with a uniform spatial distribution of the droplets. We did not observe an anisotropy of droplet shape in the probes prepared in the presence of the field. The droplet size distribution is rather narrow. The prevailed droplet diameter is about $1 \mu\text{m}$.

The director configuration inside NLC droplets with diameters of about $5 \mu\text{m}$ can be identified by observation in polarizing microscope. Such large droplets often form in the outlying parts of the PDLC layers during phase separation. The pictures typical of PDLCs formed at $U_{uv} = 0$ and 40 V are shown in figures 5(a) and (b), respectively. It is seen that the droplets are spherically shaped regardless of the field applied during phase separation. The

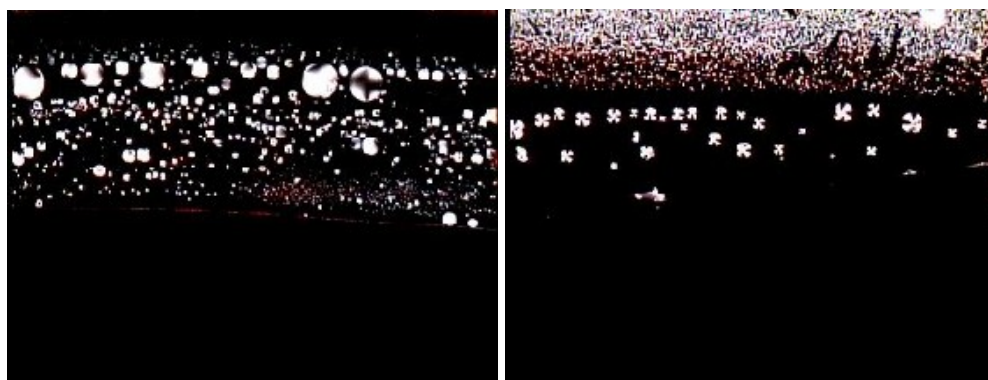
(a) $U_{uv} = 0$ V(b) $U_{uv} = 40$ V

Figure 5. Periphery part of the PDLC layers as viewed by a polarizing microscope. The layers are prepared at (a) $U_{uv} = 0$ V and (b) $U_{uv} = 40$ V. It is clearly seen that the bipolar droplets are orientationally disordered at $U_{uv} = 0$ V and are oriented along the field at $U_{uv} = 40$ V.

Table 1. Zero-field and saturated transmittance, T_0 and T_{sat} , measured at different values of the voltage U_{uv} applied during polymerization (the film thickness is $20 \mu\text{m}$ and the accuracy of the measurements is about $\pm 0.7\%$). The corresponding theoretical values of T_0 and the order parameter Q are given in the last four columns.

U_{uv} (V)	Experiment		$Q_d = 0.85$		$Q_d = 0.9$	
	T_0 (%)	T_{sat} (%)	T_0 (%)	Q	T_0 (%)	Q
0	8	97	9.0	0.04	7.0	0.05
2	10	97	10.04	0.25	10.3	0.4
10	13	90	12.9	0.4	13.0	0.49
20	40	95	39.8	0.775	40.5	0.8
50	84	99	83.5	0.96	83.6	0.97
100	88	99	87.5	0.97	89.0	0.98

bipolar structure inside the droplets can also be clearly observed. For the sample prepared at $U_{uv} = 0$, the droplets are randomly oriented, whereas the droplets in the sample obtained at $U_{uv} = 40$ V are aligned along the direction of the applied field.

For the concentrations of the components used in our samples (60 wt% of polymer and 40 wt% of NLC), the concentration of NLC droplets is not large. It is confirmed by weak scattering of light in these composites.

For PDLCs based on our components, the fractions of NLCs confined in droplets and of NLCs dissolved in the polymer matrix were obtained from IR measurements in [15]. According to these results, in our case only about 30% of the NLC phase separates. Assuming that the density of the polymer is 1.5 g cm^{-3} and the density of E7 is 1.05 g cm^{-3} , we can estimate the volume fraction of droplets, η , to be about 23.5 vol%.

The obtained data are summarized in table 1, where the values of the transmittance in the off state T_0 and the transmittance in the saturated state T_{sat} measured for different values of the voltage U_{uv} applied during phase separation. It can be concluded that the transmittance in the saturated state T_{sat} is almost insensitive to the voltage U_{uv} applied during phase separation as opposed to the initial transmittance T_0 which rapidly grows with U_{uv} and eventually saturates.

3. Theory

3.1. Model and order parameters

In this section our task is to study the problem of light scattering by an ensemble of partially ordered spherical NLC droplets dispersed in an optically isotropic polymer matrix with the dielectric constant ϵ_p and the refractive index $n_p = \sqrt{\epsilon_p}$. The ensemble of such droplets can be regarded as a reasonably simplified model of the PDLC system described in section 2.3.

In accord with our experimental results, we consider the case in which NLC is tangentially ordered at the droplet surfaces and the NLC director field $\hat{\mathbf{n}}_{LC}$ inside the droplet forms the bipolar orientational structure [19]. The symmetry of this structure is cylindrical and there are boojum surface singularities at the droplet poles defined by the symmetry (bipolar) axis of the bipolar configuration $\hat{\mathbf{n}}_d$.

The bipolar droplets are optically anisotropic with the dielectric tensor

$$\epsilon_{LC} = \epsilon_{\perp}^{(lc)} \mathbf{I} + \epsilon_a^{(lc)} \hat{\mathbf{n}}_{LC} \otimes \hat{\mathbf{n}}_{LC}, \quad (2)$$

where $\epsilon_a^{(lc)} = \epsilon_{\parallel}^{(lc)} - \epsilon_{\perp}^{(lc)}$ and \mathbf{I} is the identity matrix. Thus, the refractive indices of ordinary and extraordinary waves are $n_o^{(lc)} = \sqrt{\epsilon_{\perp}^{(lc)}}$ and $n_e^{(lc)} = \sqrt{\epsilon_{\parallel}^{(lc)}}$, respectively.

We shall also need to introduce the dielectric tensor averaged over the director distribution inside a droplet $\langle \epsilon_{LC} \rangle_{lc} \equiv V_d^{-1} \int_{V_d} \epsilon_{LC} d^3\mathbf{r} = \epsilon_d$, where V_d is the droplet volume. Owing to the cylindrical symmetry of the orientational structure, each bipolar droplet can be characterized by the nematic-like tensorial order parameter

$$\langle (3\hat{\mathbf{n}}_{LC} \otimes \hat{\mathbf{n}}_{LC} - \mathbf{I})/2 \rangle_{lc} = Q_d (3\hat{\mathbf{n}}_d \otimes \hat{\mathbf{n}}_d - \mathbf{I})/2, \quad (3)$$

so that the average dielectric tensor of a bipolar droplet ϵ_d is

$$\epsilon_d = \langle \epsilon_{LC} \rangle_{lc} = \epsilon_{\perp} \mathbf{I} + \epsilon_a \hat{\mathbf{n}}_d \otimes \hat{\mathbf{n}}_d, \quad (4)$$

where $\epsilon_{\perp} = \epsilon_{\perp}^{(lc)} + \epsilon_a^{(lc)} (1 - Q_d)/3$ and $\epsilon_a \equiv \epsilon_{\parallel} - \epsilon_{\perp} = \epsilon_a^{(lc)} Q_d$.

By analogy to the bipolar axis $\hat{\mathbf{n}}_d$, which defines the droplet orientation, the scalar order parameter Q_d will be referred to as the bipolar order parameter. This parameter characterizes the degree of droplet anisotropy that depends on distortions of the director field with respect to the uniform configuration aligned along the bipolar axis.

In general, the value of Q_d varies depending on a number of factors such as droplet size and shape, anchoring conditions, applied voltage and so on. In [20], such variations are found to be negligible and the bipolar order parameter was estimated to be about 0.82. By contrast, the results of [9, 10] suggest that the bipolar order parameter of a PDLC film can be considerably affected by an applied electric voltage.

In any event, so long as the size and shape polydispersity is weak, variations of the bipolar order parameter throughout a sample can be reasonably disregarded. On the other hand, it is now commonly accepted that disorder in positions and orientation of bipolar droplets is of vital importance for an understanding of light scattering in PDLC systems [11, 12, 21]. When the orientational distribution of the bipolar axis is uniaxial, similarly to equation (3), the average over bipolar axis orientation

$$\langle (3\hat{\mathbf{n}}_d \otimes \hat{\mathbf{n}}_d - \mathbf{I})/2 \rangle = Q (3\hat{\mathbf{N}} \otimes \hat{\mathbf{N}} - \mathbf{I})/2 \quad (5)$$

describes this distribution in terms of the order parameter Q and the optical axis $\hat{\mathbf{N}}$.

When the direction of the bipolar axis is randomly distributed, the PDLC film is isotropic and $Q = 0$. This case is illustrated in figure 1(a). The initial off state of a PDLC film is often assumed to be isotropic.

Applying an external electric field will reorient NLC inside the droplets so as to introduce an overall anisotropy of the sample with the optical axis $\hat{\mathbf{N}}$ parallel to the field. Figure 1(b) schematically shows a distribution of this sort. The limiting case where all the droplets are aligned along the field direction corresponds to the on state of a PDLC film in the regime of saturation (the saturated state) with $Q = 1$.

The effect of the order parameters Q_d and Q on light scattering in PDLC films will be our major concern.

3.2. Effective dielectric tensor

The films under consideration exemplify an inhomogeneous medium in which a host material and isolated inclusions are clearly identified. Our first step is to determine effective dielectric characteristics of the film in the long wavelength limit. To this end, we restrict ourselves to the case where the droplets are well separated and the volume fraction of droplets, η , is not too high.

Under these conditions, following [13, 22], we may use the excluded volume approximation discussed by Landauer in [23] and write the total average electric field \mathbf{E} as

$$\mathbf{E} = \eta \mathbf{E}_d + (1 - \eta) \mathbf{E}_p, \quad (6)$$

where \mathbf{E}_p and \mathbf{E}_d are the average electric fields in the polymer matrix and inside the droplets, respectively. Using the relation for the mean electric polarization vectors: \mathbf{P} , \mathbf{P}_d and \mathbf{P}_p , that can be written by analogy with equation (6), we have

$$\epsilon_{\text{eff}} \mathbf{E} = \eta \epsilon_d \mathbf{E}_d + (1 - \eta) \epsilon_p \mathbf{E}_p. \quad (7)$$

In (7) the orientationally averaged dielectric tensor (4) is used as an approximation for the dielectric tensor averaged over the droplets.

The fields \mathbf{E}_d and \mathbf{E}_p can now be related by means of an anisotropic version of the traditional Maxwell-Garnett closure [13, 22] (reviews of other approximate schemes can be found in [23–25]):

$$\mathbf{E}_p = \mathbf{M} \mathbf{E}_d, \quad \mathbf{M} = (2\epsilon_p \mathbf{I} + \epsilon_d) / (3\epsilon_p). \quad (8)$$

Combining equations (6), (7) and (8) gives the final result for ϵ_{eff} :

$$\epsilon_{\text{eff}} = \epsilon_p \mathbf{I} + \eta \langle (\epsilon_d - \epsilon_p \mathbf{I}) \mathbf{M}^{-1} \rangle [\eta \langle \mathbf{M}^{-1} \rangle + (1 - \eta) \mathbf{I}]^{-1} = \epsilon_m \mathbf{I} + \Delta \epsilon_m \hat{\mathbf{N}} \otimes \hat{\mathbf{N}}, \quad (9)$$

$$\epsilon_m = \epsilon_p \frac{\epsilon_{\perp} + 2\epsilon_p + 2\eta\epsilon_1}{\epsilon_{\perp} + 2\epsilon_p - \eta\epsilon_1} \approx \epsilon_p + \eta\epsilon_1, \quad (10)$$

$$\Delta \epsilon_m = 9\epsilon_p^2 \epsilon_a \eta \frac{\epsilon_{\perp} + 2\epsilon_p}{\epsilon_{\parallel} + 2\epsilon_p} \left[(\epsilon_{\perp} + 2\epsilon_p - \eta\epsilon_1)(\epsilon_{\perp} + 2\epsilon_p - \eta\epsilon_2) \right]^{-1}, \quad (11)$$

where $\epsilon_1 = \epsilon_{\perp} - \epsilon_p + \epsilon_p \epsilon_a (1 - Q) / (\epsilon_{\parallel} + 2\epsilon_p)$ and $\epsilon_2 = \epsilon_{\perp} - \epsilon_p + \epsilon_p \epsilon_a (1 + 2Q) / (\epsilon_{\parallel} + 2\epsilon_p)$.

For the polymer with $n_p = 1.54$ and the liquid crystal mixture E7 with $n_o^{(\text{lc})} = 1.5216$ and $n_e^{(\text{lc})} = 1.74$, it can be verified that the linear relation on the right-hand side of equation (10) gives a good approximation for the volume fraction dependence of the effective dielectric constant ϵ_m . This is a modified version of the mixing rule $\epsilon_m = (1 - \eta)\epsilon_p + \eta\epsilon_{\perp}$ used in [12].

Equation (11) clearly indicates that, in general, the anisotropic part of the effective dielectric tensor does not vanish. But the effective anisotropy parameter $\Delta \epsilon_m / \epsilon_m$ is found to be well under 0.05, so that the effective medium is weakly anisotropic as compared to NLC inside the droplets, where $\epsilon_a^{(\text{lc})} / \epsilon_{\perp}^{(\text{lc})} > 0.3$. For this reason, as in [9–12, 26], anisotropy of the effective medium can be disregarded.

In our subsequent treatment of the light scattering problem we shall use the relation (10) to account for the dependent scattering effects by replacing the polymer matrix surrounding the droplets with the effective medium. It should be noted, however, that the result (10) is strictly valid only in the Rayleigh limit where the scatterer size is much smaller than the wavelength of light (an extended discussion can be found in chapter 9 of [27]). This result can also be derived from the self-consistency condition that requires vanishing the average scattering amplitude in the forward direction for droplets embedded in the effective medium [28]. So, the effective dielectric constant (10) serves as the lowest order approximation of a coherent potential approach [29].

3.3. Light scattering and optical transmittance

In this section we begin with the light scattering problem for a single LC droplet characterized by the average dielectric tensor (4) and surrounded by the medium with the effective refractive index $n_m = \sqrt{\epsilon_m}$. Using the well-known Rayleigh–Gans approximation [30, 31], we compute the elements of the scattering amplitude matrix and the scattering cross section.

Then we apply the Percus–Yevick approximation [32, 33] to evaluate the effective scattering as the scattering cross section averaged over positions of the droplets and perform averaging of the scattering cross section over the bipolar axis orientation. Finally, in the low concentration approximation, we derive the expressions for the scattering mean free path and the optical transmittance.

3.3.1. Scattering amplitude matrix in the Rayleigh–Gans approximation. Following the standard procedure [30, 31], the undisturbed incident wave is assumed to be a harmonic plane wave with frequency ω and wavenumber $k = n_m\omega/c$. The wave is propagating through the effective medium along the direction specified by a unit vector $\hat{\mathbf{k}}_{\text{inc}}$ and the wavevector $\mathbf{k}_{\text{inc}} = k\hat{\mathbf{k}}_{\text{inc}}$. The polarization vector of the electric field is

$$\mathbf{E}_{\text{inc}} = E_i^{(\text{inc})} \hat{\mathbf{e}}_i(\hat{\mathbf{k}}_{\text{inc}}), \quad (12)$$

where the basis vectors $\hat{\mathbf{e}}_x(\hat{\mathbf{k}}_{\text{inc}}) = (\cos\theta_i \cos\phi_i, \cos\theta_i \sin\phi_i, -\sin\theta_i)$ and $\hat{\mathbf{e}}_y(\hat{\mathbf{k}}_{\text{inc}}) = (-\sin\phi_i, \cos\phi_i, 0)$ are perpendicular to $\hat{\mathbf{k}}_{\text{inc}}$ defined by the polar and azimuthal angles: θ_i and ϕ_i . (Throughout the paper summation over repeated indices will be assumed.)

Asymptotic behaviour of the scattered outgoing wave in the far field region ($kr \gg 1$) is known [30, 31]:

$$\mathbf{E}_{\text{sca}}(\mathbf{r}) \sim \mathbf{E}_{\text{sca}} \frac{e^{ikr}}{kr}, \quad \mathbf{E}_{\text{sca}} = E_i^{(\text{sca})} \hat{\mathbf{e}}_i(\hat{\mathbf{k}}_{\text{sca}}), \quad (13)$$

where $\hat{\mathbf{k}}_{\text{sca}} = \hat{\mathbf{r}} = (\sin\theta \cos\phi, \sin\theta \sin\phi, \cos\theta)$ and \mathbf{E}_{sca} is linearly related to the polarization vector of the incident wave (12) through the scattering amplitude matrix $\mathbf{A}(\mathbf{k}_{\text{sca}}, \mathbf{k}_{\text{inc}})$ in the following way:

$$E_i^{(\text{sca})} = A_{ij}(\mathbf{k}_{\text{sca}}, \mathbf{k}_{\text{inc}}) E_j^{(\text{inc})}. \quad (14)$$

The elements of the scattering amplitude matrix can be easily computed by using the Rayleigh–Gans approximation (RGA) [30, 31]. This approximation is known to be applicable to the case of submicron nematic droplets [12, 34, 35] and gives the following result:

$$A_{ij}(\hat{\mathbf{k}}_{\text{sca}}, \hat{\mathbf{k}}_{\text{inc}}) = \frac{V_d k^3}{4\pi} \hat{\mathbf{e}}_i(\hat{\mathbf{k}}_{\text{sca}}) \cdot \boldsymbol{\epsilon}(\mathbf{q}) \cdot \hat{\mathbf{e}}_j(\hat{\mathbf{k}}_{\text{inc}}), \quad (15)$$

$$\boldsymbol{\epsilon}(\mathbf{q}) = V_d^{-1} \int_{V_d} \boldsymbol{\epsilon} e^{i(\mathbf{q}\cdot\mathbf{r})} d^3\mathbf{r} = f(qR_d)\boldsymbol{\epsilon}, \quad (16)$$

$$\boldsymbol{\epsilon} = (\epsilon_d - \epsilon_m \mathbf{I})/\epsilon_m \equiv \alpha \mathbf{I} + \beta \hat{\mathbf{n}}_d \otimes \hat{\mathbf{n}}_d, \quad (17)$$

where $V_d = 4\pi R_d^3/3$ is the droplet volume; R_d is the droplet radius, $\mathbf{q} = \mathbf{k}_{\text{sca}} - \mathbf{k}_{\text{inc}}$, $f(x) = 3(\sin x - x \cos x)/x^3$, $\alpha \equiv \epsilon_{\perp}/\epsilon_m - 1$, $\beta \equiv \epsilon_a/\epsilon_m$.

3.3.2. Scattering cross section. All scattering properties of a droplet can be computed from the elements of the scattering amplitude matrix (15). In particular, when the incident wave is unpolarized, it is not difficult to deduce the expression for the differential scattering cross section characterizing the angular distribution of the scattered light:

$$\sigma_{\text{diff}} = \frac{A_d(kR_d)^4}{18\pi} F(qR_d) \psi_{ij} \psi_{ij}, \quad \psi_{ij} = \hat{\mathbf{e}}_i(\hat{\mathbf{k}}_{\text{sca}}) \cdot \boldsymbol{\epsilon} \cdot \hat{\mathbf{e}}_j(\hat{\mathbf{k}}_{\text{inc}}), \quad (18)$$

where $F(qR_d) = f^2(qR_d)$ is the form factor and $A_d = \pi R_d^2$ is the area of the droplet projection onto the plane normal to $\hat{\mathbf{k}}_{\text{inc}}$.

The RGA scattering cross section (18) depends on droplet orientation only through the last factor which can be rewritten in the following form:

$$\psi_{ij} \psi_{ij} \equiv \psi^2 = \text{Tr } \boldsymbol{\epsilon}^2 + [\hat{\mathbf{k}}_{\text{sca}} \boldsymbol{\epsilon} \hat{\mathbf{k}}_{\text{inc}}]^2 - \hat{\mathbf{k}}_{\text{inc}} \boldsymbol{\epsilon}^2 \hat{\mathbf{k}}_{\text{inc}} - \hat{\mathbf{k}}_{\text{sca}} \boldsymbol{\epsilon}^2 \hat{\mathbf{k}}_{\text{sca}}. \quad (19)$$

Substituting the tensor (17) into equation (19) yields the orientationally dependent factor in the explicit form:

$$\begin{aligned} \psi^2 = & \alpha^2 [1 + (\hat{\mathbf{k}}_{\text{inc}} \cdot \hat{\mathbf{k}}_{\text{sca}})^2] + [\alpha + \beta]^2 - \alpha^2] \\ & \times [1 - (\hat{\mathbf{k}}_{\text{inc}} \cdot \hat{\mathbf{n}}_d)^2 - (\hat{\mathbf{k}}_{\text{sca}} \cdot \hat{\mathbf{n}}_d)^2] + [\beta (\hat{\mathbf{k}}_{\text{inc}} \cdot \hat{\mathbf{n}}_d) (\hat{\mathbf{k}}_{\text{sca}} \cdot \hat{\mathbf{n}}_d)]^2 \\ & + 2\alpha\beta (\hat{\mathbf{k}}_{\text{inc}} \cdot \hat{\mathbf{k}}_{\text{sca}}) (\hat{\mathbf{k}}_{\text{inc}} \cdot \hat{\mathbf{n}}_d) (\hat{\mathbf{k}}_{\text{sca}} \cdot \hat{\mathbf{n}}_d). \end{aligned} \quad (20)$$

This result will be used to perform orientational averaging of the scattering cross section.

3.3.3. Scattering mean free path. Our task now is to evaluate the scattering mean free path, l_{sca} , which is also known as the phase coherence length or the extinction length [29, 36]. This is the characteristic distance between two scattering events after which the phase coherence of radiation gets lost leading to the exponential decay of the incident intensity known as the Lambert–Beer law [37, 38]. So, the optical transmittance through a film of thickness d is given by

$$T_{\text{sca}} = \exp(-d/l_{\text{sca}}). \quad (21)$$

So long as the volume fraction is not too high, the scattering mean free path can be derived by using the low concentration approximation. The result is

$$l_{\text{sca}}^{-1} = n \int \sigma_{\text{eff}} d\hat{\mathbf{k}}_{\text{sca}}, \quad (22)$$

where $d\hat{\mathbf{k}}_{\text{sca}} \equiv \sin \theta d\theta d\phi$ and $n = \eta/V_d$ is the number density of the droplets. In the limit of weak size and shape polydispersity, we define the effective cross section σ_{eff} as the single scattering cross section (18) averaged over both positions and orientation of bipolar droplets:

$$\sigma_{\text{eff}} = \langle \langle \sigma_{\text{diff}} \rangle \rangle = \frac{A_d(kR_d)^4}{18\pi} F(qR_d) \langle \langle \psi^2 \rangle \rangle, \quad (23)$$

where R_d is now the mean value of the droplet radius. In order to avoid ambiguity, we shall denote averages over droplet type by $\langle \langle \dots \rangle \rangle$ and averages over bipolar axis orientation by $\langle \dots \rangle$.

When positional and orientational degrees of freedom are statistically independent, the result of averaging over positional disorder is known to be a sum of two terms describing the coherent and the incoherent scattering [12, 33, 39]. So, we have

$$\langle \langle \psi^2 \rangle \rangle \equiv \Psi = \Psi_{\text{coh}} + \Psi_{\text{incoh}}, \quad \Psi_{\text{coh}} = S(\mathbf{q}) \langle \psi \rangle^2, \quad \Psi_{\text{incoh}} = \langle \psi^2 \rangle - \langle \psi \rangle^2, \quad (24)$$

where the contributions to the coherent and the incoherent scattering are proportional to Ψ_{coh} and Ψ_{incoh} , respectively; $S(\mathbf{q}) = 1 + n \int e^{i(\mathbf{q}\cdot\mathbf{r})} [g(\mathbf{r}) - 1] d^3\mathbf{r}$ is the structure factor expressed in terms of the pair correlation function $g(\mathbf{r})$ [33].

The coherent part of Ψ describes light scattering by a positionally disordered ensemble of identical droplets. The scattering properties of each droplet are now characterized by the orientationally averaged tensor (17):

$$\langle \epsilon \rangle = \bar{\alpha} \mathbf{I} + \bar{\beta} \hat{\mathbf{N}} \otimes \hat{\mathbf{N}} = [\alpha + \beta(1 - Q)/3] \mathbf{I} + \beta Q \hat{\mathbf{N}} \otimes \hat{\mathbf{N}} \quad (25)$$

and we obtain $\langle \psi \rangle^2$ from the expression (20) modified as follows

$$\begin{aligned} \langle \psi \rangle^2 &= \bar{\alpha}^2 [1 + (\hat{\mathbf{k}}_{\text{inc}} \cdot \hat{\mathbf{k}}_{\text{sca}})^2] + [(\bar{\alpha} + \bar{\beta})^2 - \bar{\alpha}^2] \\ &\quad \times [1 - (\hat{\mathbf{k}}_{\text{inc}} \cdot \hat{\mathbf{N}})^2 - (\hat{\mathbf{k}}_{\text{sca}} \cdot \hat{\mathbf{N}})^2] + [\bar{\beta} (\hat{\mathbf{k}}_{\text{inc}} \cdot \hat{\mathbf{N}}) (\hat{\mathbf{k}}_{\text{sca}} \cdot \hat{\mathbf{N}})]^2 \\ &\quad + 2\bar{\alpha}\bar{\beta} (\hat{\mathbf{k}}_{\text{inc}} \cdot \hat{\mathbf{k}}_{\text{sca}}) (\hat{\mathbf{k}}_{\text{inc}} \cdot \hat{\mathbf{N}}) (\hat{\mathbf{k}}_{\text{sca}} \cdot \hat{\mathbf{N}}). \end{aligned} \quad (26)$$

When the structure factor equals unity, $S(\mathbf{q}) = 1$, the droplets are positionally uncorrelated. This approximation, however, cannot be appropriate for the morphology, where the droplets do not overlap. As in [12], in order to take into account droplet self-avoidance, we shall use the structure factor for binary mixtures of hard spheres computed from the exact solution of the Percus–Yevick equation [32, 33]. The structure factor expressed in terms of the Ornstein–Zernike direct correlation function $c(r)$ is given by [40–42]

$$S(\mathbf{q}) = S_{\text{PY}}(qR_d) = \frac{1}{1 - nC(\mathbf{q})}, \quad C(\mathbf{q}) = \int_{r \leq 2R_d} e^{i(\mathbf{q}\cdot\mathbf{r})} c(r) d^3\mathbf{r}, \quad (27)$$

where $c(r) = 6\eta\gamma_1(r/2R_d) - \gamma_2[1 + \eta/2(r/2R_d)^3]$, $\gamma_1 = (1 + \eta/2)^2/(1 - \eta)^4$ and $\gamma_2 = (1 + 2\eta)^2/(1 - \eta)^4$.

Droplet orientation fluctuations induce the incoherent scattering described by Ψ_{incoh} in (24). The expression for Ψ_{incoh} can be derived in the following form

$$\begin{aligned} \Psi_{\text{incoh}} &= \frac{\beta^2}{9} (1 - Q) [3(1 + Q) - (1 - Q) (\hat{\mathbf{k}}_{\text{inc}} \cdot \hat{\mathbf{k}}_{\text{sca}})^2] \\ &\quad + \beta^2 \left[\langle (\hat{\mathbf{k}}_{\text{inc}} \cdot \hat{\mathbf{n}}_d)^2 (\hat{\mathbf{k}}_{\text{sca}} \cdot \hat{\mathbf{n}}_d)^2 \rangle - \langle (\hat{\mathbf{k}}_{\text{inc}} \cdot \hat{\mathbf{n}}_d)^2 \rangle \langle (\hat{\mathbf{k}}_{\text{sca}} \cdot \hat{\mathbf{n}}_d)^2 \rangle \right], \end{aligned} \quad (28)$$

where $\langle (\hat{\mathbf{k}}_{\text{inc(sca)}} \cdot \hat{\mathbf{n}}_d)^2 \rangle = Q (\hat{\mathbf{k}}_{\text{inc(sca)}} \cdot \hat{\mathbf{N}})^2 + (1 - Q)/3$. In accordance with the above interpretation, equation (28) shows that the incoherent scattering is solely caused by the anisotropic part of the droplet dielectric tensor and disappears when the droplets are perfectly aligned with $Q = 1$. In addition to the order parameter Q , there are fourth order averages in the last square bracketed term on the right-hand side of (28) and we need to know additional higher order parameters to estimate the incoherent scattering.

The special case in which both the incidence direction and the optical axis of the film are normal to the substrates, $\hat{\mathbf{k}}_{\text{inc}} = \hat{\mathbf{N}} = \hat{\mathbf{e}}_z$, is of particular interest. In this case the above results take the simplified form:

$$\Psi_{\text{coh}}(\theta) = \bar{\alpha}^2 S(\mathbf{q}) [1 + \cos^2 \theta], \quad (29)$$

$$\Psi_{\text{incoh}}(\theta) = \frac{\beta^2}{9} (1 - Q) [3(1 + Q) - (1 - Q) \cos^2 \theta] + \beta^2 \frac{3 \cos^2 \theta - 1}{2} [\langle n_z^4 \rangle - \langle n_z^2 \rangle^2], \quad (30)$$

where $\cos \theta = (\hat{\mathbf{k}}_{\text{sca}} \cdot \hat{\mathbf{e}}_z)$ and $n_z = (\hat{\mathbf{n}}_d \cdot \hat{\mathbf{e}}_z)$.

We can now combine equations (22)–(24) and the relations (29) and (30) to obtain the ratio of the droplet radius R_d and the scattering mean free path l_{sca} :

$$R_d/l_{\text{sca}} = \frac{\eta(kR_d)^4}{12} \int_{-1}^1 F(qR_d) \Psi(\theta) d(\cos \theta), \quad (31)$$

where $q^2 = 2k^2(1 - \cos \theta)$.

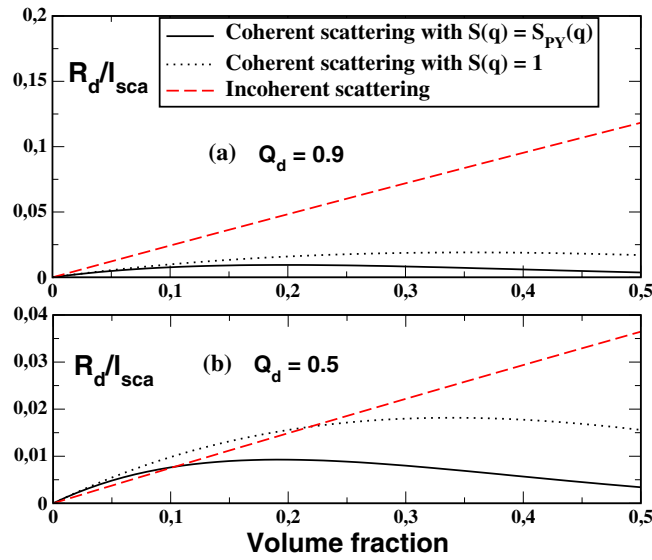


Figure 6. Coherent and incoherent light scattering contributions to the ratio R_d/I_{sca} versus the volume fraction η at $R_d = 0.5 \mu\text{m}$ for two values of the bipolar order parameter Q_d : (a) $Q_d = 0.9$ and (b) $Q_d = 0.5$. Refractive indices used in calculations are: $n_p = 1.54$, $n_o^{(lc)} = 1.52$ and $n_e^{(lc)} = 1.74$.

3.4. Numerical results

Optical transmittance of a normally incident unpolarized light through a film can be computed from (21) combined with the formulae (27) and (29)–(31).

Figure 6 shows that correlations in droplet positions generally reduce the incoherent scattering as compared to the case of positionally uncorrelated droplets. This effect becomes more pronounced as the bipolar order parameter decreases. Referring to figure 6(a), the incoherent scattering dominates at relatively large bipolar order parameters and, as is seen from figure 6(b), this is no longer the case for weakly anisotropic droplets.

Dependencies of the optical transmittance on the bipolar order parameter for different droplet radii are given in figure 7. When the angular distribution of the bipolar axis is isotropic and $Q = 0$, figure 7(a) shows that the transmittance declines as Q_d increases. Such behaviour is mainly due to an increase in the incoherent scattering governed by the anisotropic part of the tensor (17). The latter is the ratio $\beta = \epsilon_a/\epsilon_m$ that characterizes anisotropy of the bipolar droplets and grows with the bipolar order parameter.

In the opposite case of perfectly aligned droplets with $Q = 1$, shown in figure 7(b), the incoherent scattering is suppressed. It is seen that the transmittance reaches its maximal value at $Q_d \approx 0.8$ where the refractive index of the effective medium n_m and the ordinary refractive index of the droplets $n_o = \sqrt{\epsilon_{\perp}}$ are matched. Equivalently, from equation (29) the coherent scattering disappears when the matching condition: $\bar{\alpha} = 0$ is fulfilled.

Computing the dependence of the transmittance on the order parameter Q requires the knowledge of the variance $\langle n_z^4 \rangle - \langle n_z^2 \rangle^2$ that enters the factor (30) describing the incoherent scattering. The variance of n_z^2 cannot be negative and vanishes at both $Q = 1$ and $-1/2$. In addition, it equals $4/45$ in the isotropic state with $Q = 0$.

For simplicity, we suppose that the orientational distribution can be parameterized by the order parameter Q and approximate the variance by the simple polynomial with a maximum

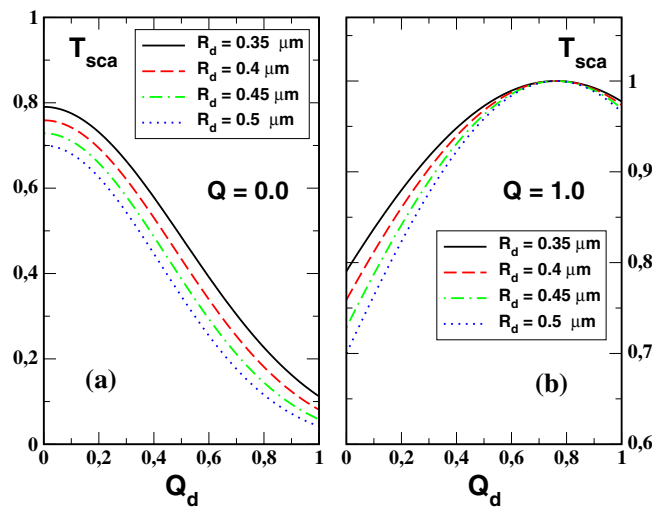


Figure 7. Transmittance as a function of the bipolar order parameter Q_d at the volume fraction $\eta = 0.235$ for different droplet radii and two values of the order parameter Q : (a) $Q = 0$ and (b) $Q = 1$.

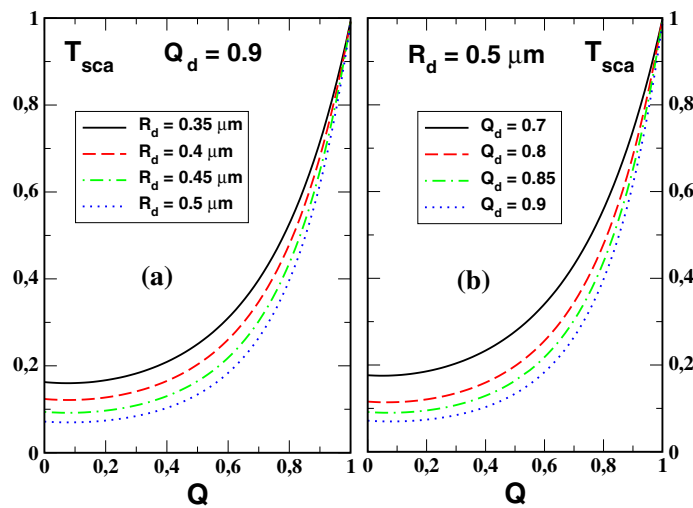


Figure 8. Transmittance as a function of the order parameter Q at (a) various values of the mean droplet radius R_d for $Q_d = 0.9$ and at (b) various values of the bipolar order parameter Q_d for $R_d = 0.5 \mu\text{m}$. The droplet volume fraction is 0.235 and the thickness of PDLC layer is $20 \mu\text{m}$.

at $Q = 0$: $\langle n_z^4 \rangle - \langle n_z^2 \rangle^2 \approx 4(1 - Q)^2(2Q + 1)/45$. The results of numerical calculations are presented in figure 8.

4. Discussion

Dependencies of the transmittance on the order parameter Q plotted in figure 8(b) can be used to estimate the values of Q and Q_d from the transmission coefficient measured in the zero-

field and saturated states, T_0 and T_{sat} , of PDLC films prepared in the presence of an electrical field. The first column of table 1 gives the voltage U_{uv} applied across the film of the PDLC precursor during UV polymerization. This voltage affects the ordering of the droplets, and the experimental results for T_0 and T_{sat} are listed in the second and third columns, respectively.

According to table 1, the smallest value of T_0 , $T_0 \approx 0.08$, corresponds to the sample prepared in the absence of external fields. Theoretically, this value can be estimated as the minimal transmittance of the T_{sca} versus Q curve. Referring to figure 8(b), this transmittance depends on the bipolar order parameter Q_d . The theoretical results are found to be in agreement with the experimental value $T_0 \approx 0.08$ at Q_d ranged between 0.85 and 0.9. So, the bipolar order parameter appears to be close to the estimate of [20], $Q_d \approx 0.82$.

We also found that the order parameter Q corresponding to the transmittance T_0 at $U_{\text{uv}} = 0$ is very small ($Q \approx 0.04$). This result supports the commonly accepted assumption that PDLC films prepared with no applied voltage are nearly isotropic.

When $U_{\text{uv}} \neq 0$ and Q_d is known, the initial transmittance T_0 and the order parameter Q can be evaluated from the corresponding T_{sca} versus Q curve. For $Q_d = 0.85$ and 0.9, the results are given in the last four columns of table 1. The order parameter is shown to be an increasing function of U_{uv} . When the voltage U_{uv} increases, the value of Q rapidly grows and saturates.

It should be emphasized that, in addition to the order parameters Q_d and Q , there are a number of parameters that enter the theory. For these parameters we have used the values estimated from the experimental data. These are: the refractive indices of the polymer ($n_p = 1.54$) and the liquid crystal ($n_o^{(\text{lc})} = 1.52$ and $n_e^{(\text{lc})} = 1.74$), the thickness of the film ($d = 20 \mu\text{m}$), the mean value of the droplet radius ($R_d = 0.5 \mu\text{m}$) and the volume fraction of droplets ($\eta = 0.235$).

Finally, we comment on limitations of our theoretical treatment that essentially relies on the Rayleigh–Gans approximation to describe light scattering in terms of the order parameters. It is, however, applicable only for sufficiently small droplets when $|n_{o,e}/n_m - 1| \ll 1$ and $kR_d|n_{o,e}/n_m - 1| \ll 1$.

The single scattering by larger droplets has been previously studied by using the anomalous diffraction approach [43] and the T -matrix theory [44]. In these more complicated cases averaging over droplet orientation will require the knowledge of additional higher order averages characterizing orientational distribution of the droplets. Nevertheless, as can be concluded from the experimental data of section 2, the Rayleigh–Gans approximation is acceptable provided the droplet radius is below $0.7 \mu\text{m}$.

We have also used the effective medium theory combined with the low concentration approximation. For optically isotropic scatterers, such a mixed approach is known to provide reasonably accurate results when the volume fraction is under 0.3 [36]. Otherwise, a more sophisticated treatment of multiple scattering effects is required.

5. Conclusion

In this study we have considered light scattering in PDLC composites with the ‘Swiss cheese’ morphology in relation to the orientational order parameters of bipolar droplets. We have applied the theoretical approach based on the Rayleigh–Gans approximation to estimate the order parameters from the experimental results on light transmittance through the samples.

It is shown that the droplet ordering can be controlled by applying an electrical field during phase separation. This ordering increases with the voltage and saturates. In the samples prepared in the absence of the field, the droplets are found to be almost randomly distributed.

Acknowledgments

This study was carried out under the project ‘Ordering regularities and properties of nano-composite systems’ supported by the National Academy of Sciences of Ukraine. We also thank O Lavrentovich and Liou Qiu (Liquid Crystal Institute, Kent State University) for assistance with SEM measurements.

References

- [1] Doane J W 1990 *Liquid Crystals—Application and Uses* vol 1, ed B Bahadur (Singapore: World Scientific) p 361
- [2] Drzaic P S 1995 *Liquid Crystal Dispersions* (Singapore: World Scientific)
- [3] Crawford G P and Žumer S (ed) 1996 *Liquid Crystals in Complex Geometries* (London: Taylor and Francis)
- [4] Higgins D A 2000 *Adv. Mater.* **12** 251
- [5] Sutherland R L, Tondiglia V P, Natarajan L V, Bunning T J and Adams W W 1994 *Appl. Phys. Lett.* **64** 1074
- [6] Penterman R, Klink S I, de Koning H, Nisato G and Broer D J 2002 *Nature* **417** 55
- [7] Margerum D, Lackner J, Ramos E, Lim K and Smith W 1985 *Liq. Cryst.* **5** 1477
- [8] Wu J J and Wang C M 1997 *Phys. Lett. A* **232** 149
- [9] Bloisi F, Terrecuso P, Vicari L and Simoni F 1995 *Mol. Cryst. Liq. Cryst.* **266** 229
- [10] Bloisi F, Ruocchio C, Terrecuso P and Vicari L 1996 *Opt. Commun.* **123** 449
- [11] Kelly J R and Palffy-Muhoray P 1994 *Mol. Cryst. Liq. Cryst.* **243** 11
- [12] Cox S J, Reshetnyak V Y and Sluckin T J 1998 *J. Phys. D: Appl. Phys.* **31** 1611
- [13] Levy O 2000 *Phys. Rev. E* **61** 5385
- [14] Bhargava R, Wang S Q and Koenig J L 1999 *Macromolecules* **32** 2748
- [15] Bhargava R, Wang S Q and Koenig J L 1999 *Macromolecules* **32** 8989
- [16] Bhargava R, Wang S Q and Koenig J L 1999 *Macromolecules* **32** 8982
- [17] Dolgov L and Yaroshchuk O 2003 *Proc. SPIE* **5257** 48
- [18] Zakrevska S, Zakrevskyy Y, Nych A, Yaroshchuk O and Maschke U 2002 *Mol. Cryst. Liq. Cryst.* **375** 467
- [19] Ondris-Crawford R, Boyko E P, Wagner B G, Erdmann J H, Žumer S and Doane J W 1991 *J. Appl. Phys.* **69** 6380
- [20] Reshetnyak V Y, Sluckin T J and Cox S J 1997 *J. Phys. D: Appl. Phys.* **30** 3253
- [21] Žumer S, Golemme A and Doane J W 1989 *J. Opt. Soc. Am. A* **5** 403
- [22] Cox S J, Reshetnyak V Y and Sluckin T J 1996 *J. Phys. D: Appl. Phys.* **29** 2459
- [23] Landauer R 1978 *Electrical Transport and Optical Properties of Inhomogeneous Media (AIP Conf. Proc.* vol 40) ed J C Garland and D B Tanner (New York: American Institute of Physics) pp 2–43
- [24] van Beek L K H 1967 *Progress in Dielectrics* vol 7, ed J B Birks (London: Heywood) pp 69–114
- [25] Bergman D J and Stroud D 1992 *Solid State Phys.* **46** 147
- [26] Basile F, Bloisi F, Vicari L and Simoni F 1993 *Phys. Rev. E* **48** 432
- [27] Mishchenko M I, Hovenier J W and Travis L D (ed) 2000 *Light Scattering by Nonspherical Particles: Theory, Measurements and Applications* (New York: Academic)
- [28] Stroud D and Pan F P 1978 *Phys. Rev. B* **17** 1602
- [29] Soukoulis C M, Datta S and Economou E N 1994 *Phys. Rev. B* **49** 3800
- [30] Ishimaru A 1978 *Wave Propagation and Scattering in Random Media* (New York: Academic)
- [31] Newton R G 1982 *Scattering Theory of Waves and Particles* 2nd edn (Heidelberg: Springer)
- [32] Percus J K and Yevick G J 1958 *Phys. Rev.* **110** 1
- [33] Ziman J M 1979 *Models of Disorder: The Theoretical Physics of Homogeneously Disordered Systems* (Cambridge: Cambridge University Press)
- [34] Žumer S and Doane J W 1986 *Phys. Rev. A* **34** 3373
- [35] Leclercq L, Maschke U, Ewen B, Coqueret X, Mechernene L and Bermouna M 1999 *Liq. Cryst.* **26** 415
- [36] Busch K, Soukoulis C M and Economou E N 1994 *Phys. Rev. B* **50** 93
- [37] Sheng P 1995 *Introduction to Wave Scattering, Localization and Mesoscopic Phenomena* (New York: Academic)
- [38] van Rossum M C W and Nieuwenhuizen T M 1999 *Rev. Mod. Phys.* **71** 313
- [39] Lax M 1951 *Rev. Mod. Phys.* **23** 287
- [40] Thiele E 1963 *J. Chem. Phys.* **39** 474
- [41] Wertheim M S 1963 *Phys. Rev. Lett.* **39** 474
- [42] Lebowitz J L 1964 *Phys. Rev. A* **133** 895
- [43] Žumer S 1988 *Phys. Rev. A* **37** 4006
- [44] Kiselev A D, Reshetnyak V Y and Sluckin T J 2002 *Phys. Rev. E* **65** 056609